Applied Geochemistry 203 (2026) 106807

Contents lists available at ScienceDirect

Applied Geochemistry

journal homepage: www.elsevier.com/locate/apgeochem

The role of organic matter in the colloid mobility and solid-liquid distribution of naturally abundant lanthanides and actinides: Case of the Boom Clay formation

Muriel Bouby [a,*], Ugras Kaplan [a,1], Frank W. Geyer [a], Alexander Lunz [a], Horst Geckeis [a], Stéphane Brassinnes [b]

[a] Karlsruhe Institute of Technology (KIT), Institute for Nuclear Waste Disposal (INE), Karlsruhe, D-76021, Germany
[b] ONDRAF/NIRAS, Belgian Agency for Radioactive Waste and Enriched Fissile Materials, Geological Disposal, R&D, Avenue des Arts, 14, Bruxelles, 1210, Belgium

ARTICLE INFO

Editorial handling by: Elisa Sacchi

Keywords:
Boom clay (BC)
Dissolved organic matter (DOM)
Pore waters (PW)
Asymmetrical flow field-flow fractionation (AsFlFFF)
Liquid chromatography-organic carbon detection (LC-OCD)
ICP-MS
OM-Colloid mobility
Impact of leachable OM on lanthanide and actinide retention

ABSTRACT

In Belgium, deep geological disposal of radioactive waste is envisaged in poorly indurated clay formations like the Boom Clay (BC). In the present work we applied the Asymmetrical Flow Field-Flow Fractionation coupled to a UV-Vis spectrophotometer (AsFlFFF-UV) as well as the Liquid Chromatography coupled to Organic Carbon Detection, UV and ICP-MS (LC-OCD-UV-ICP-MS) to study dissolved organic matter (DOM) mobility. Small sized DOM fractions (<7 nm) are detected in all BC porewaters (BCPW) where the maximum of the species size distribution is at a hydrodynamic diameter of ~1.8-1.9 nm. Pore waters originating from or influenced by the double band (DB) structure exhibit a multimodal size distribution ranging to larger sized colloidal entities up to ~30 nm. The findings support the outcome of earlier investigations stating that the inter layer mobility of DOM in BC apparently is restricted to species with a diameter of <7 nm. Trace elements (Fe, Mn, Ni, lanthanides, Th, U) reveal a variable and complex association with colloidal species in BCPW and BC leachates where FeOOH/DOM aggregates play a role. An attempt is made to derive so-called *in-situ* $K_{d(OM)}$-values i.e. the distribution of naturally abundant lanthanides and actinides between dissolved OM in BCPW and OM being extractable from solid BC samples by a leaching step using 15 mM $NaHCO_3$ solution. Results are compared with laboratory K_d-values described in the literature and point to the significant contribution of the immobile OM to lanthanide and actinide retention.

1. Introduction

Natural organic matter (NOM) is ubiquitous in the environment, occurring in all soils, waters, and sediments (Aiken et al., 1985; Suffet et al., 1989; Davies et al., 1998; Ghabbour et al., 2000; Clapp et al., 2001). It possesses a large variety of properties coming from its detrital nature, its origin from various sources (e.g. marine and terrestrial reservoirs), and its different formation pathways (degradation, oxidation, polymerisation, …). NOM is therefore heterogeneous by definition related to size, elemental composition, structure, and functional entities (Swift, 1999; Piccolo, 2001; Simpson et al., 2002; Sutton et al., 2005). Humic substances refer to that part of NOM, which has already undergone severe transformation and decomposition after deposition. The NOM in Boom Clay can be classified as consisting solely of humic substances considering the formation pathways and the diagenetic history. The fraction of the NOM pool, which can be solubilised in aqueous solution is referred to as dissolved organic matter (DOM). DOM is subdivided into humic and fulvic acids. Humic acids (HA) are insoluble at acidic pH values (pH < 2) but are soluble for higher pH values (Aiken et al., 1985). HA are typically composed of larger macromolecules. Fulvic acids (FA) are soluble in water at all pH values and are composed of smaller molecules (Aiken et al., 1985). For more than three decades, HA and FA are the most studied fractions of NOM in soil science due to their ability to complex radionuclides (RNs) and toxic metals (Kim et al., 1987; Moulin et al., 1992; Choppin, 1992; McCarthy et al., 1998; Geckeis et al., 2003; Suteerapataranon et al., 2006; Reiller et al., 2012;

This article is part of a special issue entitled: Migration 2025 published in Applied Geochemistry.

* Corresponding author.
E-mail address: muriel.bouby@kit.edu (M. Bouby).
[1] present address: Los Alamos National Laboratory, Carlsbad, New Mexico 88220, United States.

https://doi.org/10.1016/j.apgeochem.2026.106807
Received 7 January 2026; Received in revised form 25 March 2026; Accepted 30 March 2026
Available online 1 April 2026

Maes et al., 2011).

Poorly indurated clay formations like the Oligocene Boom Clay (BC) are envisaged by the Belgian Agency for Radioactive Waste and enriched Fissile Material (ONDRAF/NIRAS) as a possible deep geological host formation for radioactive waste disposal. Compared to other argillaceous formations studied in the European context of radioactive wastes geological disposal, the BC contains substantial amounts of organic matter (OM) of low maturity (total organic carbon (TOC) content 1-5 wt %). The NOM pool is distributed between the liquid and the solid phase. The BC OM was already subject of detailed petrographic (Vandenberghe, 1978) and geochemical studies (Laenen, 1997). Overviews of BC OM and their characteristics are available from e.g. (Van Geet et al., 2003). Recent studies focused on "undisturbed" samples typical for the Mol-Dessel region (Belgium) (Deniau et al., 2001; Blanchart et al., 2012). The results of around 200 analyses show that the present day BC pore water (BCPW) at the Mol site is a dilute $NaHCO_3$ solution of 10-20 mM with a pH slightly above 8, a negative E_h potential (−200 to −400 mV) and containing a significant amount of dissolved organic carbon (88 ± 67 mgC/L) (Wang et al., 2023; Honty et al., 2022) (see Table 1). The Na^+, Cl^-, I^- concentrations and alkalinity increase with the depth of the BC layer over a thickness of 65 m around the underground laboratory (HADES URL, Mol, Belgium) located at 200 m below sea level. The water type and the concentration profile observed in the upper (meteoric) and lower (marine type) aquifers create a concentration gradient which consistently explains these trends, thus interpreted as diffusion-controlled transport of originally marine BC pore water after sea regression and further sediment burial (Wang et al., 2023).

The determination of any variability in the concentration and the size distribution of BC DOM collected from the HADES URL, Mol, Belgium has been subject of detailed studies (Durce et al., 2015, 2016, 2018). They show that due to its low maturity and relatively high O/C ratio, the total OM pool is able to generate a relatively high concentration of DOM in BCPW with mostly less than 10 nm (hydrodynamic diameter) in size, even though only less than 0.2% of the total organic matter content (TOC) in the BC is found dissolved in BCPWs. Only a DOM size fraction with hydrodynamic diameter <6 nm was found to be mobile (Durce et al., 2015) due to the confined pore structure of the Boom Clay at the Mol-Dessel reference site where the HADES URL is located, with a BC pore throat diameter determined at 6.6-7.6 nm (Durce et al., 2018), i.e. the diameter of those pores in the sedimentary rock, which is available for colloids or macromolecules to pass. Leaching DOM from BC samples in the laboratory generates larger species and accounts for approximately 12 % of the TOC (Durce et al., 2015). The TOC content (and to a lesser extent the hydrogen index of the kerogen) controls the concentration of the leachable DOM (Durce et al., 2015). The high fraction of leachable TOC consisting of relatively larger sized DOM entities as compared to the BCPW DOM points to the preferential retention or filtration of large sized organic macromolecules leaving only smaller ones in pore waters. Only in those layers consisting of siltier and/or sandy layers, also larger sized DOM species can be mobile (Durce et al., 2015).

Previous size characterization of DOM was carried out by using the size exclusion chromatography (SEC) technique coupled to a UV-Visible spectrophotometer used at a fixed detection wavelength (280 nm) (Durce et al., 2015, 2016, 2018). SEC in general provides a high size resolution (Pelekani et al., 1999; Perminova et al., 2003; Striegel et al., 2009; Chin et al., 1994), however, exhibits in many cases a limited working range so that some material is eluted directly at the "so-called" exclusion limit, as observed in (Durce et al., 2015). Detailed information on the larger sized DOM fractions could often thus not be obtained.

In the present work we used the asymmetrical flow field-flow fractionation (AsFlFFF), coupled on-line to a UV-Vis detector and liquid (size exclusion) chromatography (LC) with organic carbon, UV-Vis and ICP-MS detection. Both methods can be flexibly operated to analyse colloidal material with broad size distributions (see e.g. (Giddings et al., 1976; Beckett et al., 1987; Schimpf and Petteys, 1997; Schimpf et al., 2000; Ngo Manh et al., 2001; Huber et al., 1991; Huber et al., 2011; Tasi et al., 2024)). The application of ICP-MS as a detector allows for the multi-element analysis in colloidal matter as a function of colloid diameter (Taylor et al., 1992; Hasselöv et al., 1999; Bouby et al., 2008, 2012). We specifically looked at naturally abundant trace elements like U, Th and the lanthanides in different DOM samples in order to draw conclusions on the potential behaviour of radioactive waste derived radionuclides in BC systems. Samples were BC pore waters extracted from various piezometer filters installed at the HADES underground lab in Mol, Belgium and DOM released from solid BC samples by leaching. The aim of the study is related to three topics:

- Identification of the potential inter layer mobility of measured colloidal species and associated metal ions.
- Characterization of the BC colloid composition including trace inorganic components.
- Quantification of the naturally abundant lanthanide, U and Th distribution between BC porewater and Boom Clay leachate solutions and derive estimates for the role of immobile clay mineral associated OM for lanthanide and actinide retention.

2. Material and methods

The pore waters and solid clay samples were provided by Euridice, a general Partnership between ONDRAF/NIRAS, the Belgian Agency for

Table 1
BCPW composition.

mg/L	BCPW at the Mol site[a]	SPRING[b]		SPRING[c]	Morpheus F4[c]	Morpheus F8[c]	Morpheus F12[c]	Morpheus F20[c]
pH lab.[d]	8.5 ± 0.4			8.80 ± 0.01	8.73 ± 0.01	8.80 ± 0.02	8.82 ± 0.03	8.78 ± 0.01
E_h lab.[d] (mV)	−220 to −400			−170 ± 20	−188 ± 50	−227 ± 50	−197 ± 50	−203 ± 30
Na	308 ± 58	298	390	302 ± 2.2 %	314 ± 3.1 %	275 ± 1.5 %	351 ± 1.7 %	314 ± 2.5 %
K	8 ± 2	8.7	12.0	6.8 ± 3.0 %	7.5 ± 3.9 %	7.36 ± 0.6 %	7.31 ± 2.1 %	5.4 ± 3.8 %
Mg	1.7 ± 0.6	1.9	4.0	3.0 ± 1.1 %	1.5 ± 0.2 %	1.78 ± 1.5 %	2.33 ± 2.7 %	1.73 ± 1.2 %
Ca	2.4 ± 1	2.2	4.7	2.7 ± 0.7 %	1.3 ± 1.4 %	1.82 ± 1.2 %	2.07 ± 0.6 %	1.47 ± 0.3 %
Fe	0.3 ± 0.4	0.3	1.2	0.4 ± 1.2 %	0.26 ± 0.2 %	1.02 ± 0.8 %	0.30 ± 0.2 %	0.22 ± 1.6 %
Al	0.05 ± 0.04			<0.04	<0.04	0.07 ± 3.7 %	<0.04	<0.04
Si	5 ± 3	2.6	4.5	4.6 ± 0.2 %	5.9 ± 1.3 %	5.6 ± 1.1 %	5.9 ± 0.7 %	5.4 ± 1.3 %
F^-	2.4 ± 0.7	2.6	2.9	2.78 ± 0.02 %	2.46 ± 4.2 %	3.22 ± 0.3 %	2.77 ± 0.01 %	2.46 ± 0.32 %
Cl^-	20 ± 5	18.5	24.8	19.4 ± 0.5 %	19.2 ± 4.6 %	29.3 ± 2.1 %	23.3 ± 2.5 %	21.5 ± 1.1 %
SO_4^{2-}	2 ± 2	<0.25	4.2	0.16 ± 17 %	0.79 ± 9.7 %	0.49 ± 40 %	0.58 ± 7.1 %	1.54 ± 3.6 %
DOC	88 ± 67	n/a		71 ± 7.0 %	76 ± 6.6 %	131 ± 35 %	87 ± 15 %	85 ± 33 %

[a] Mean values derived from 195 water samples (Wang et al., 2023; Honty et al., 2022).
[b] Data from (De Craen et al., 2004).
[c] This work.
[d] As determined in the Ar glove box just after the opening of the Swagelok containers.

Radioactive waste and Enriched Fissile Materials, and SCK.CEN in charge of the management of the HADES underground research laboratory (URL) (Mol, Belgium) (see (Van Geet et al., 2023) for the HADES URL history).

2.1. Pore water samples: BCPW

Boom Clay pore water (BCPW) samples come from two piezometers, namely Spring (TD-116E) and Morpheus (TD-11D). The sampling campaign was done in October 2023. A detailed description of these piezometers can be found in (De Craen et al., 2004, 2019). Samples were taken in Argon pre-flushed stainless-steel containers (Swagelok®). This sampling procedure preserves the original waters and protect them from photodegradation (Lou et al., 2006). The containers were kept in an Ar glove box. One sample from Spring, and four from Morpheus, namely from the filters -F4, -F8, -F12 and -F20 were analyzed between February 2024 and October 2024.

Spring (drilled in October 1999) is a piezometer made of stainless steel (SS) casing and SS AISI 316L (Krebsöge, SIKA R5, material: 1.4404) filters with a pore size between 7 and 16 μm (Honty et al., 2022; De Craen et al., 2019) placed horizontally in the BC and is located in the Test Drift part of the HADES URL (ring 116) at ~ 223 m below surface level (BSL) It is entirely made of stainless steel and equipped with four large filter screens, representing in total about 6 m collection, and pointing towards the east. The hydraulic interconnections of this substantial length result in a high-water flow (~350 mL per day). The water was collected in October 2023 with all filters connected.

Morpheus (drilled in May 2001) is a vertically oriented piezometer designed to study the variability of the BC pore water composition (especially the BC organic matter and the elemental content) underneath the HADES URL (Honty et al., 2022; De Craen et al., 2019). It allows the sampling at 12 distinct stratigraphic levels of the BC such as: organic rich layers, carbonate rich layers, more silty layers, and the level of the so-called "double-band (DB)" consisting on two very silty layers rich in organic content. The Morpheus piezometer casing is made of hardened PVC and Schumaterm 20 (sintered mullite, porcelainite) filter screens with an average pore diameter of 15 μm (Honty et al., 2022; De Craen et al., 2019). The collection setup guarantees a sampling with only limited geochemical disturbances. The Morpheus filter 8 (Morpheus-F8) provides pore water from the DB silty layer, where the hydraulic conductivity is two or three times higher than for the rest of the BC. Physically and chemically, the water collected is influenced largely by the characteristics of the DB layer.

According to Hemes et al., 2013, 2015, Boom clay is characterized by a complex pore structure with pore sizes ranging from the nm to the μm scale showing a strong anisotropy of the pore space connectivity. Durce et al. (2015) conclude from percolation experiments pore throats around 6-8 nm perpendicular to the clay rock bedding. Cut-offs of the filter screens are clearly larger than those so that pore size exclusion or filtration effects related to the pore size of the filter screens can be neglected (Honty et al., 2022).

2.2. Sediment material

2.2.1. Description

Sediment materials come from a so-called "cutting-edge" sample cored in January 2006 vertically down to the HADES URL gallery, perpendicular to the bedding plane (*cutting edge 06/52/Test Drift/Ring 25-26/3.65 m to 4 m below the HADES URF (intrados)*). The cutting edges were immediately sealed off with flanges and stored at 4 °C. Boom Clay samples obtained by cutting edges have a minimal excavation disturbed zone (EDZ) due to the high plasticity, and only the open sides of the cylinder have been in contact with oxygen for a short period before sealing. The clay cylinder has been extruded out of the tube on January 2010 and cut in small disc pieces of ~40 mm and ~15 mm in length and vacuum repacked in Al-PE foil (SIF, Fig. SIF-1 up). This operation was done under atmospheric conditions (short time period 1-2 h). Oxidation of the outer surface has therefore taken place. Samples were stored in a fridge until use in summer 2013.

The horizon where samples are taken from is similar to that of the Spring piezometer, i.e. in the median plane of HADES-URL. According to (Durce et al., 2015), TOC of BC at this position is ~1 wt%.

2.2.2. Leaching tests: instantaneous OM release

As oxidation of the outer surface has taken place, the outer „oxidized" rim (~2 mm) of a clay disc is removed with a knife which is easily done due to the high clay plasticity. Then some inner-pieces are suspended for 1 week under atmospheric conditions in a synthetic Boom Clay water (SBCW) consisting of 15 mM $NaHCO_3$ at a solid/liquid ratio of 0.2 kg/L (SIF, Fig. SIF-1 middle). The suspension obtained from this leaching experiment is distributed in small Eppendorf tubes (2 mL) and ultra-centrifuged (centrifuge SIGMA, Germany) at 15,000 rpm ($g_{max} = 16162$) for 90 min. For reproducibility tests, the mobilized entities, i.e. the supernatant (BC extract) called hereafter BC leachates (SIF, Fig. SIF-1 bottom) from three clay discs (CD) was collected and stored in tight glass vials at 4 °C in the dark prior to the analysis under aerobic conditions.

2.3. Analysis of BCPW and BC leachates

BCPW and BC leachates were analyzed by ICP-MS (THERMO Scientific, iCAP TQ, Germany). Sample solutions were acidified (3 % HNO_3). In order to analyse lanthanides at lowest concentrations, special care was taken to clean the sample introduction system with ultrapure HNO_3 solution, in order to minimize background signals and detection limits. In order to avoid sedimentation of flocculated humic acid, samples were agitated shortly prior to the injection into the nebulizer.

Respective detection limits for Fe, U, Th, Ce and Lu (the latter two taken as representatives for light and heavy lanthanide elements), were at 0.2 μg/L, 0.1 ng/L, 0.8 ng/L, 0.03 ng/L and 0.03 ng/L, respectively.

The non-purgeable (i.e. non-volatile) organic carbon (NPOC) content of the BC leachates and BCPW samples was determined (TOC analyser, TOC-L, Shimadzu) after a 1:20 or a 1:10 dilution in ultra-pure water (Millipore, Merck, Germany).

For the Morpheus BCPW samples we noticed high NPOC values analyzed by the TOC analyzer, being clearly higher than the LC-OCD data. We assume contaminations of low molecular weight organic components (e.g. softeners) from the piezometer (Schumaterm filters or PVC or nylon or new inline particles filters) being responsible for this deviation. We, therefore, took only the NPOC due to macromolecular constituents as determined by LC-OCD.

The concentrations of the main anions (F^-, Cl^-, SO_4^{2-}) were determined by Ion Chromatography (ICS-3000, column AS9 HC, Thermo Scientific, Germany).

pH values for each BCPW were determined in an Ar glove box (semi-micro electrode Orion 8103BN and Orion 720A pH-meter). E_h was monitored in the Ar glove box (redox combination electrode BlueLine 31RX, SI Analytics, Germany) just after the opening of the Swagelok containers.

2.3.1. Sample conditioning

Before analysis by AsFlFFF and LC, aliquots of the various BCPW samples were taken out from the corresponding Swagelok container stored in the Ar-glove box.

For the AsFlFFF, 3 times 1 mL of each BCPW, were placed in glass vials closed hermetically with a septum in the Ar glove box. The vials were then transferred to the auto-sampler of the AsFlFFF. A small amount of the original BCPW is injected (100 μL) without any pre filtration 3 times consecutively for each BCPW from the 3 independent vials.

For the LC, 20 mL of each BCPW sample were placed in glass vials closed with a pre-cut household aluminum foil (3 × 3 cm in size) secured

with a holed screw cap. The needle of the auto-sampler perforated the vials. Accordingly, the vials and its content are only preserved for air contact (and thus oxygen access) until the first aspiration and injection. Six successive injections of 1 mL sample volume each were performed.

The BC leachates, preserved in a fridge since their preparation, are diluted by 10 in the eluent prior to injection in the AsFlFFF system (100 μL) or in the LC system (1 mL).

2.3.2. AsFlFFF and LC system principle; ICPMS coupling

The AsFlFFF used in this study (AF2000 MultiFlow FFF Series) is provided by Postnova analytics, Landsberg, Germany (SIF, Fig. SIF-2). It works similarly to the previous model (HRFFF 10.000) we described in detail in our former work (Bouby et al., 2008, 2011; Gopalakrishnan et al., 2023). A brief overview is given in the SIF (see Fig. SIF-2 and the corresponding text).

The LC-OCD-UVD-OND (see SIF, Fig. SIF-3) is a liquid chromatography (size-exclusion chromatography, SEC) setup coupled on-line to an organic carbon detector (OCD), a UV-Vis detector (UVD) and an organic nitrogen detector (OND). This method is described in detail in (Huber et al., 2011; Tasi et al., 2024) and www.doc-labor.de. The method allows for the separation of NOM into major fractions of different sizes and chemical functions, the identification of various compound classes (biopolymers, humic substances (HS), low molecular weight compounds …) and the quantification of colloid bound, organic and inorganic nitrogen. A brief overview is given in the SIF (see Fig. SIF-3 and the corresponding text).

The additional coupling to an Inductively Coupled Plasma Mass Spectrometer (ICP-MS) allows the detection of the inorganic elements associated to the individual compounds (fractions), at trace levels. More details are given in the SIF (see Fig. SIF-4 and the corresponding text).

2.3.3. Size/molecular weight (MW) calibration

The AsFlFFF and the LC/SEC are both sized-based fractionation techniques, separating the components in a flowing liquid. AsFlFFF coupled to UV/Vis detection (λ = 225 nm) fractionates colloids according to their sizes in a laminar flow profile in a thin channel with an applied cross flow according to their different diffusion coefficients. Small colloids are eluted first followed by larger sized particles. In LC-OCD-UV separation of colloid sizes is achieved in a porous medium, where larger colloidal particles are excluded from the medium pores and, thus, elute first followed by smaller sized particles.

The conversion of the time for the elution of individual particles into a size or molecular weight (MW) information is done with colloid reference standards. For humic like colloids it has been recommended to use monodisperse sodium polystyrene sulfonate (Na-PSS) standards (Beckett et al., 1987). Note that while MW is generally well defined, the random-coiled structures of humic/fulvic acids and Na-PSS may change according to the pH or the ionic strength (Swift, 1999; Beckett et al., 1987; Schimpf and Petteys, 1997; Ghosh et al., 1980; Avena et al., 1999; Berden et al., 1990; Chin et al., 1991; Kirkland et al., 1992; Moon, 1995; Moon et al., 2006; Schimpf et al., 1997) so that hydrodynamic diameters may vary to different degrees for individual species in different media.

In the present work we used 15 mmol/L $NaHCO_3$ solution (pH = 8.4) as carrier or eluent solution throughout most of the analyses, as it mimics the BCPW composition as observed at Mol (Honty et al., 2022; De Craen et al., 2004). In order to convert the certified MW of Na-PSS standards into the respective hydrodynamic diameter relevant for given solution composition, a survey of the literature was done for that purpose. Wijhoven et al. (Wijnhoven et al., 1995), Reszat et al. (2009), Durce et al. (2015) used eluents at IS varying from 10 up to 20 mM. Their data were all taken in a single fit to obtain an equation to correlate the Na-PSS MW to their size (see Figure SIF-5 in the SIF). The corresponding equation is the following:

$$log(d_S) = 0.13(\pm 0.03) + 0.57(\pm 0.01)^{*}log(MW) \quad \text{(equation 1)}$$

with d_s the hydrodynamic diameter (Stokes diameter) expressed in nm and MW the molecular weight in kDa.

Those data were taken to calculate hydrodynamic diameters in our experiments with 15 mmol/L $NaHCO_3$ solution as a carrier solution. We add for comparison the data from Ngo Manh et al. (Ngo Manh et al., 2001) acquired using a 5 mmol/L Tris-buffer eluent (pH = 9.4). The corresponding equation is the following:

$$log(d_S) = 0.274(\pm 0.001) + 0.580(\pm 0.001)^{*}log(MW) \quad \text{(equation 2)}$$

with d_s the hydrodynamic diameter (Stokes diameter) expressed in nm and MW the molecular weight in kDa.

The lower IS and higher pH of this eluent apparently induces an expansion of the PSS structure and thus lead to an increasing hydrodynamic diameter. From Figure SIF-5 it becomes also obvious that size variations for colloidal matter at a given MW become larger for larger sized colloids and are less relevant for particles with sizes at around 1 nm.

In the present work, a series of polystyrene sulfonate (PSS) reference standards (Polysciences, Eppelheim, Germany) of different molecular weights ((MW): 0.891, 1.67, 3.42, 6.43, 15.8, 33.5, 65.4, and 148.5 kDa) are used for size calibration of the AsFlFFF and LC-OCD-UVD. The AsFlFFF calibration was completed by a series of carboxylated polystyrene reference particles (Magsphere, USA) of different sizes (diameters: 21, 103, and 190 nm given by the manufacturer).

Using equation (1) and the elution times of each Na-PSS standards at their peak maximum, it is possible to estimate the sizes corresponding to the various elution times at which the analytes present in the BCPW are detected (as reported in Figs. 1 and 2).

3. Results

3.1. Composition of BCPW and BC extracts

Cation and anion concentrations in the different BCPW samples and extracts are shown in Tables 1 and 2. Main pore water components and parameters (Na^+, K^+, Ca^{2+}, Cl^-, F^-, SO_4^{2-}, E_h and pH) are similar for the BCPWs collected from various horizons of the Boom Clay lithostratigraphy (see assignment of samples to different layers in (Wang et al., 2023; De Craen et al., 2019)). Differences appear, however, in concentrations of DOC, Fe and of various trace elements. Notably in the Morpheus-F8 samples, concentrations of DOC, Fe and trace elements such as lanthanides, U and Th are significantly higher than in other samples. Our values lie consistently within the range of hitherto reported data for pore water samples from EG/BS (another piezometer sampling in the DB) and SPRING (Wang et al., 2023; Honty et al., 2022; De Craen et al., 2004). DOC in the BC extracts (clay discs leachates samples) is obtained in a single leaching step and is at 59 to 84 mg_C/L (Table 2). This concentration lies in the same range as reported by Durce et al., 2015) (Durce et al., 2015), who performed leaching in an Ar flushed glove box, and corresponds to ca. 0.3-0.4 g C $(kg\ rock)^{-1}$. Note, that this is much less (i.e. 2-4%) than the total organic carbon (TOC) in the BC layer where the sediment sample comes from (acc. to Durce et al., 2015 this at about 1-1.5 wt%). Durce et al., 2015 performed multiple leaching steps and report that about 12% of the TOC can be extracted (Durce et al., 2015).

Separate ICP-MS measurements were performed for the analysis of the entire series of lanthanides, uranium and thorium in Morpheus-F4, -F8, -F12, -F20 and the BC leachates. Special care was taken to attain highest detection sensitivity and low background in order to be able to quantify also the heavy lanthanides being abundant at only ng/L concentration levels (see Table 3). Those data are used to compare and interpret lanthanide pattern as discussed below.

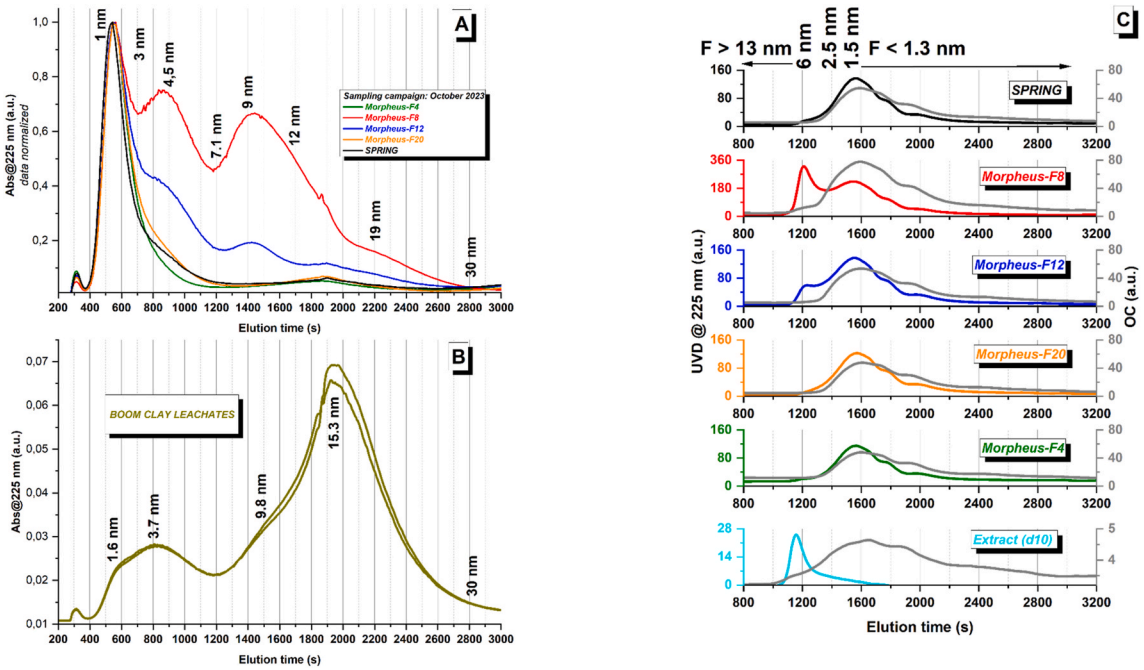

Fig. 1. AsFlFFF-UVD and LC-OCD-UVD measurements done for all BCPW in $NaHCO_3$ 15 mM as eluent; A: AsFlFFF-UVD for all BCPW; B: AsFlFFF-UVD for the BC leachates; C: LC-OCD- UVD for all the BCPW and the BC leachates. F in the size scale at the top of each figure stands for size "Fraction". In the LC-OCD chromatograms in C, 13 nm (1150 s) corresponds to the exclusion limit of the column and 1.3 nm to the lower end of the calibration range.

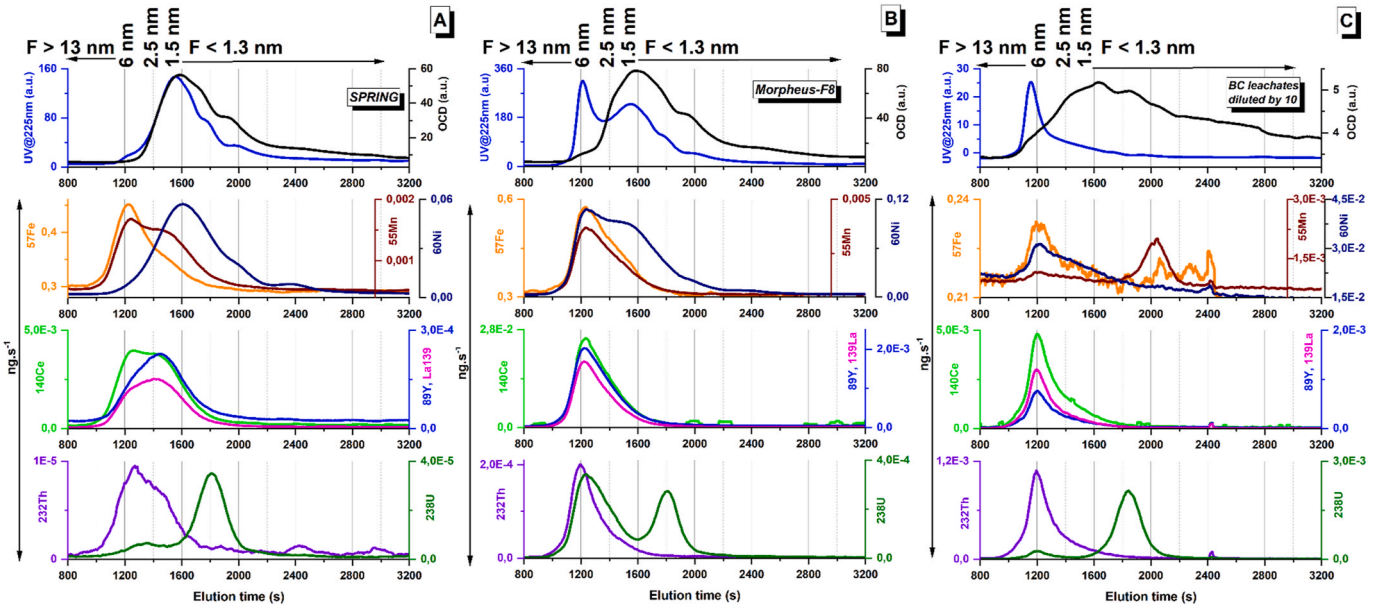

Fig. 2. LC-OCD-UVD-ICPMS-chromatograms as obtained after injection of the various BCPW: A: SPRING, B: Morpheus-F8 and C: BC leachates. Injection volume: 1 mL; Eluent $NaHCO_3$ 15 mM. F in the size scale at the top of each figure stands for size "Fraction". In the LC-OCD chromatograms , 13 nm (1150 s) corresponds to the exclusion limit of the column and 1.3 nm to the lower end of the calibration range.

3.2. Size characterisation of dissolved organic matter (DOM)

The size distribution of DOM in pore water and BC leachate samples is analyzed by AsFlFFF coupled to UV/Vis detection ($\lambda = 225$ nm) and LC-OCD-UV where beside UV/Vis detection also the very sensitive organic carbon detector (OCD) is coupled. Results are summarized in Fig. 1. Note, that replicate fractograms and chromatograms for all samples are very reproducible.

Fig. 1 (left side, top for the BCPW (A) and bottom for the BC leachates (B) samples) shows the original normalized AsFlFFF-UV-fractograms. The maximum of the DOM size distribution found by AsFlFFF for all BCPWs is at a hydrodynamic diameter of ~1.5 nm. At the relatively high IS of the carrier solution, an overloading effect as e.g. described by Ngo Manh et al. (Ngo Manh et al., 2001) who used a low IS and high pH carrier solution, should not exert a relevant effect. We nevertheless performed dilution experiments (i.e. dilution factors from 10 to 360) and found a slight effect resulting in a shift of the size distribution by ~0.3-0.4 nm so that the real size of the main fraction in all BCPW samples should be rather at 1.8-1.9 nm. For Morpheus-F4, -F20 and SPRING, only one main DOM fraction is detected where the size

Table 2
Composition of BC leachates.

mg/L	Leachate 1	Leachate 2	Leachate 3
Na	390 ± 4.0 %	339 ± 1.9 %	347 ± 4.3 %
K	18.8 ± 7.3 %	11.1 ± 5.7 %	11.1 ± 8.6 %
Mg	4.5 ± 4.1 %	*3.2* ± 2.1 %	*3.1* ± 1.5 %
Ca	1.7 ± 8.8 %	1.3 ± 7.9 %	1.3 ± 8.5 %
Fe	0.39 ± 2.8 %	0.52 ± 3.8 %	0.44 ± 1.8 %
Si	11.1 ± 23 %	n/a	n/a
Al	0.13 ± 6.5 %	0.24 ± 3.3 %	0.27 ± 3.5 %
TIC	192 ± 0.2 %	149 ± 0.2 %	140 ± 0.2 %
DOC	59 ± 2.0	84 ± 1.3	83 ± 0.9

distribution tailing ranges up to ~7 nm. SPRING shows a somewhat narrower size distribution but with a more pronounced shoulder at ~4.5 nm. However, the DOM size distribution in Morpheus-F12 and notably Morpheus-F8 presents two well-resolved elution bands at larger colloid sizes (~4.5 nm and ~9.3 nm) and sizes range up to ~ 30 nm.

The sizes of the two first fractions at ~1.8-1.9 and ~4.5 nm are in the range usually reported for fulvic and humic acids (Swift, 1999; Schimpf and Petteys, 1997; Ngo Manh et al., 2001; Reszat et al., 2009; Thurman et al., 1982; Gaffney et al., 1996; Lead et al., 2000; Siripinyanond et al., 2002; Kawahigashi et al., 2005; d'Orlyé et al., 2008; Roger et al., 2010). Larger size fractions >7 nm point to the presence of larger aggregates. This is consistent with the positions of the stratigraphic layers where the Morpheus-F12 and –F8 are sampled, i.e. close to or at the so-called double band (DB), this silty layer, where the hydraulic conductivity is two or three times higher than for the rest of the BC and which may carry bigger-sized material. Those results are in line as well with those obtained previously at SCK•CEN (Honty et al., 2022).

Results of LC-OCD analysis (Fig. 1C) widely confirm the outcome of AsFlFFF experiments The OCD signals also show a maximum at a size ~ 1.5 nm for colloids consisting of organic carbon and are quite congruent with UV-chromatograms for all BCPWs. A shoulder at ~3 nm is visible for Morpheus-F8 and Morpheus-F12. Striking is the high UV-signal close to and at the exclusion limit of the size-exclusion column (i.e. ≥ ~6 nm) for Morpheus-F8 and -F12, which is much less pronounced in the OCD chromatogram where only a small shoulder is visible in this region. This might be explained by the occurrence of larger-sized organic/inorganic aggregates being visible in the UV-detector via light scattering. Note that the intensity of the light scattering signal is extremely sensitive to the increase of particle size and is proportional to the sixth power of the diameter (Müller et al., 1996). The nature and possible origin of those colloids will be discussed below (section 3.3).

Fractograms and chromatograms of the BC leachates obtained from leaching clay discs differ significantly from those of BCPWs (Fig. 1B and C). A small-sized fraction with a maximum at ~1.6 nm and somewhat larger (~3.8 nm) is also visible like in BCPW samples. However, the main fraction appears in the larger colloid size region with a broad distribution up to 30 nm and a maximum at ~15 nm. In a separate test, the BC leachates were passed through membrane filters with a nominal cutoff of 100 kDa (corresponding to an operationally defined hydrodynamic diameter of ~7 nm according to (Millipore, 2000)). AsFlFFF-UV analysis of the filtrate (see SIF, Figure SIF-7) confirms that the larger sized colloid fraction seen in the fractograms is indeed removed. Results of ultrafiltration and AsFlFFF-UV analysis consistently show the predominant presence of a large-sized colloid fraction ≥ ~6 nm, visible by the light-scattering signal in the UV/Vis detector. This again is consistent with the observation of Durce et al. (2015). LC-OCD-UV data are consistent with the outcome of AsFlFFF-UV.

3.3. *Fe, Mn, Ni, Y, lanthanide, Th in BC samples*

Fig. 2 shows the LC-OCD-UV-ICP-MS-chromatograms obtained after injection of BCPW (Spring, Morpheus-F8) and BC leachates. Elements

Table 3
Lanthanide, actinide concentrations in BCPWs (Sample, 2023) and in BC leachates (Sample, 2013).

µg/L	Morpheus F4	Std %	Morpheus F8	Std %	Morpheus F12	Std %	Morpheus F20	Std %	Spring	Std %	Leachate 1	Std %	Leachate2	Std %	Leachate 3	Std %
La	0.027	2.0	0.284	1.1	0.089	3.2	0.056	1.2	0.033	2.3	33.5	0.9	39.8	4.15	43.3	0.96
Ce	0.084	2.8	0.731	1.4	0.206	2.1	0.145	1.8	0.093	1.7	101	0.9	119.2	1.31	127.1	3.79
Pr	0.009	4.9	0.090	2.3	0.025	3.3	0.017	3.6	0.009	1.3	9.7	1.9	12.0	0.77	12.9	0.95
Nd	0.041	5.7	0.363	1.4	0.109	2.3	0.078	3.4	0.038	4.5	36.0	1.4	44.4	1.47	49.1	0.34
Sm	0.011	5.7	0.081	2.3	0.029	5.8	0.020	5.5	0.010	4.0	6.4	0.2	7.9	1.35	9.0	1.92
Eu	0.002	4.1	0.021	1.9	0.009	5.1	0.005	4.3	0.003	3.5	1.3	1.7	1.7	1.35	2.0	1.44
Gd	0.014	2.2	0.086	2.1	0.036	4.8	0.021	1.9	0.013	4.2	4.8	0.4	6.2	1.49	7.7	0.09
Tb	0.002	6.8	0.015	1.8	0.007	3.3	0.004	4.6	0.002	5.4	0.9	1.0	1.2	3.01	1.5	1.88
Dy	0.014	3.0	0.096	1.8	0.047	2.5	0.023	4.8	0.016	4.0	3.8	2.2	4.8	2.86	5.5	2.58
Ho	0.003	4.4	0.022	2.2	0.011	3.7	0.005	3.5	0.004	4.2	0.7	0.4	0.8	4.68	0.9	4.25
Er	0.012	3.7	0.077	1.8	0.040	3.5	0.018	2.9	0.014	3.0	1.9	4.6	2.4	3.03	2.8	1.40
Tm	0.002	6.0	0.012	2.2	0.006	5.1	0.003	3.2	0.002	4.0	0.2	5.2	0.3	6.53	0.3	1.79
Yb	0.013	6.5	0.088	1.9	0.047	1.2	0.019	3.7	0.015	2.7	1.3	3.3	1.6	3.10	1.9	2.34
Lu	0.002	3.5	0.016	2.8	0.009	3.5	0.004	6.5	0.003	3.6	0.2	5.0	0.3	3.95	0.3	3.58
Th	0.010	6.4	0.167	1.8	0.026	4.6	0.014	2.1	0.014	3.0	39.8	3.1	48.2	1.84	49.4	1.95
U	0.047	3.6	0.378	1.0	0.244	2.1	0.079	1.7	0.034	2.0	70.3	3	60.7	2.77	60.9	2.75

detected in the ICP-MS chromatograms are selected as being representative for pore water constituents such as Fe, Mn and the trace elements Ni, Y, La, Ce, Th and U considered as naturally abundant chemical analogues to radionuclides contained in radioactive waste.

Looking to the distribution of metal ions within the colloid size range provides interesting and diverse details. In Spring samples, most metal ions are associated with the main DOM fraction with colloid sizes <2 nm. This is not surprising, as it is well known that polyvalent metal ions notably those with oxidation states III and IV strongly interact with humic/fulvic acids under natural conditions forming fulvate/humate complexes (see e.g. (Vandenberghe, 1978)).

However, the size distributions of DOM associated Fe, Mn, Y, La, Ce and Th species are always shifted and skewed towards larger sizes (see Fig. 2), as compared to the DOC size distribution, to a different extent. This might be interpreted as a preferential complexation of inorganic elements by larger sized OM fractions or can be attributed to some kind of metal induced agglomeration effect (see discussion in (Geckeis et al., 2003; Suteerapataranon et al., 2006; Geckeis et al., 2002)). Striking is, however, that Fe appears to be predominantly associated with a size fraction close or above the exclusion limit of the column together with significant fractions of Mn, Ce, Th. Metal association with the large size fraction $\geq$ ~6 nm becomes even more pronounced for Morpheus-F8, which contains the highest DOC but also the highest Fe-concentration ($1.8{\cdot}10^{-5}$ mol/L in Morpheus-F8 compared to $7.1{\cdot}10^{-6}$ mol/L in Spring). Still 3.5-7.5% of the DOM in the BCPW appears in the chromatogram region where iron is eluted. If we translate this into a mass ratio of C to Fe, we come to a value for $R_{C/Fe}$ of ~6 to ~10 (corresponding to molar C/Fe ratios of 29-45). The large sized colloids, thus, are still mainly composed of organic carbon.

Fe and Mn exhibit a pronounced redox activity and exist under oxidizing conditions as Fe(III) and Mn(IV), respectively. Under the reducing conditions of the undisturbed BC system ($E_h = -266$ mV (Wang et al., 2023) to ≤ -270 mV (De Craen et al., 2004),). both elements are assumed to occur in their reduced forms (Fe(II) and Mn(II)). De Craen et al. report that Fe^{2+} in BCPW is in equilibrium with pyrite and siderite (De Craen et al., 2004). Divalent cations are assumed to show in general a somewhat weaker interaction with fulvic/humic acid as compared to polyvalent cations such as thorium and lanthanides. Therefore, it would be expected that divalent Fe(II) and Mn(II) should rather show a pattern like the non-redox active Ni(II). The fact that in our study, both elements are clearly associated to larger sized colloids suggests that oxidized Fe(III) and Mn(IV) species prevail. Even though BCPW samples were taken, transported and stored under anaerobic conditions, no measures were taken for the exclusion of oxygen during size fractionation with LC-OCD-UV-ICP-MS (as also reported in (Durce et al., 2015) for SEC analysis). Therefore, oxidation of at least a part of initially present Fe(II) to Fe(III) and precipitation of larger sized FeOOH/humic agglomerates cannot be excluded and may incorporate at least parts of trace metal ions such as lanthanides and Th during formation.

Separate formation of inorganic FeOOH nanoparticles in the presence of humic matter is not to be expected. Association of humic matter to Fe(III) oxihydroxides is well known and has been observed in various studies (see e.g. (Benedetti et al., 2003; Wang et al., 2020)). Therefore, the formation of FeOOH humic agglomerates are most likely responsible for the observation of the peaks at the exclusion limit, which is most evident for Morpheus-F8, containing the highest Fe-concentration.

Similar observations were made for BC leachates (Fig. 2 C). A clear association of metal ions to the larger sized colloidal fraction with significant inorganic content is found. The signal for Fe is rather noisy, due to the low Fe concentration in the 1:10 diluted leachate. As discussed already in the case of BCPW analyses, the main component of the larger colloid size fraction still is organic carbon. Values for the mass ratio $R_{C/Fe}$ in this case lie in a range of ~7 (corresponding to a molar ratio of ~33).

Whether such type of colloidal FeOOH humic aggregates observed in all samples play as well a role under the genuine, reducing BC conditions needs to be further studied. However, following the arguments in ref. (De Craen et al., 2004), we tend to assume that those large-sized FeOOH based colloid species are formed artificially as a consequence of oxygen contact during sampling, sample preparation and analysis.

The association of metal ions to different size fractions of BC DOM and OM in BC extracts was also investigated by Bruggeman et al. (2010). They found by sequential ultrafiltration, that Eu(III) added at trace concentrations ($3.2 \cdot 10^{-8}$ to $5.8 \cdot 10^{-7}$ mol/L) to BCPW (containing DOM) is distributed in a bimodal fashion in size fractions from < 1 kDa to 19 kDa and 30 – 300 kDa (~1.3 to 7.2 nm and 9.3-34.7 nm, respectively according to equation (1)). Adding Eu(III) to a BC extract results in a distribution of only a minor Eu(III) amount bound to the smaller size fraction (<1 kDa – 19 kDa) and the majority being associated with the fraction with sizes ranging from 19 to 220 nm. Taking into account, that sequential ultrafiltration does not allow for a highly resolved size distribution, their results are very consistent with the outcome of the present study when looking to the chromatograms of the naturally abundant lanthanides La and Ce. It is worth to note, that different to the present work, the experiments in (Bruggeman et al., 2010) were performed under anoxic conditions.

3.4. U in BC samples

The observed chromatograms for uranium require separate discussion. LC-OCD-ICP-MS chromatograms show in all BCPW and BC extract samples an elution band with a maximum at 1800 s for uranium which is consistent with the chromatogram of a 15 mM $NaHCO_3$ solution containing U(VI) in absence of DOM (see SIF, Fig SIF-8). This finding suggests the presence of U(VI) carbonate complexes. Note that the elution peak for uranium carbonate complexes appears outside the calibration range for the LC-column and corresponds to a size clearly <1.3 nm which nevertheless is compatible with the dimensions of uranyl carbonate complexes as obtained by EXAFS studies (see e.g. (Ikeda et al., 2009)). A part of uranium appears in the BC extract and in all BCPW samples, most pronounced in Morpheus F8, in the larger sized colloid fraction.

Carbonate apparently acts as a strong competitor ligand for U(VI) competing with fulvic/humic acid complex formation. Salah et al. (Wang et al., 2020) assume that CO_3^{2-} complexation dominates U(VI) speciation in BC pore water forming predominantly $UO_2(CO_3)_3^{4-}$ as well as minor contributions of $CaUO_2(CO_3)_3^{2-}$ and $Ca_2UO_2(CO_3)_3$(aq) complexes. While the existence of U(VI) is comprehensible under the aerobic conditions of our analytical experiments, the presence of U(IV) under the reducing conditions in genuine BCPW is also possible. Salah et al. suggest in their report that U(VI) carbonate complexes exist in equilibrium with U(IV) solid phases in the BC system (Salah et al., 2015). (Bruggeman and Maes, 2017) argue that the behaviour of uranium in transport and batch experiments under BC conditions rather points to the presence of U(IV). The elution pattern reveals in addition that at least a part of the uranium exists colloid-borne, possibly partly as a residual fraction of U(IV). Therefore, we also assume that under the genuine reducing BC conditions, U might to a significant extent exist in redox state (IV). This aspect calls for further investigations.

4. Discussion on colloid and trace element mobility

4.1. Colloid mobility

Assessing the potential mobility of DOM in BC is of interest in the context of radioactive waste disposal because DOM may act as a carrier for radionuclide migration susceptible to reduce retention. An important barrier function of clay rock consists in the nano porosity, which limits advective groundwater flow perpendicular to the layering. Mobility of colloidal OM depends on the connected porosity and the pore size distribution of the rock and physical, chemical retention at the rock surface.

Durce et al. (2015) reported recently a threshold of 20 kDa corresponding to a hydrodynamic diameter of 5.6 nm to be considered as the cut-off above which DOM species are hardly mobile in BC. In a percolation experiment, the transport of DOM in a solid sample from the HADES underground facility was studied perpendicular to the bedding plane (Durce et al., 2015). A one-dimensional reactive transport model was developed to account for the DOM retardation, diffusion and entrapment (attachment and/or straining). The value of the BC pore throat diameter deduced from this work was 6.6 to 7.6 nm. Below this threshold, DOM mobility depends on size and only for species with a molecular weight below 2 kDa significant trapping could not be observed anymore. LC-OCD-UV measurements obtained in the present work show that all BCPW samples contain DOM species with hydrodynamic diameters <7 nm while the clearly dominating small size fraction is at 1.8-1.9 nm. Following the conclusions of Durce et al. (2015), most of the DOM in BCPW is considered mobile perpendicular to BC layers. The size range in Morpheus-F8 and -F12 extends to larger sizes up to 30 nm. Morpheus-F8 water originates from the silty layers of the DB structure and contains the highest NPOC ranging up to 131 $mg_C L^{-1}$ (see Table 1), where the concentration is found to vary temporarily. The higher porosity and larger pore sizes of the silty DB layer is believed to be responsible for the higher mobility of also larger sized OM colloids within the layer in horizontal direction as observed for Morpheus-F8. Morpheus-F12 water comes from a filter, which is very close to the DB layer and most likely receives part of the pore water from this layer.

As discussed before, the BC leachates contain a large colloid fraction with sizes ranging up to 30 nm. The fact that the larger size fractions in pore water from the DB structure and in the leachates are not visible in the other samples originating from adjacent BC layers (see Fig. 1 A and C) supports the assumption, that they are not able to cross clay layers in a perpendicular direction.

Those conclusions are supported by the results of Li et al. (Yu et al., 2013) and Hemes et al., 2013, 2015. Li et al. (Yu et al., 2013) determined the geometric mean of the vertical (K_v) and horizontal (K_h) hydraulic conductivities for the Putte and Terhagen Members at the Mol site to be 1.7 10^{-12} and 4.4 10^{-12} m/s, respectively, with a vertical anisotropy K_h/K_v of about 2.5. In the siltier zones above and below the Putte and Terhagen Members higher K values are reported (but still low at 10^{-12} to 10^{-10} m/s). Hemes et al., 2013, 2015 showed a strong anisotropy of the pore space connectivity, i.e. the BC pore throats are preferentially orientated parallel to the bedding planes, suggesting a higher permeability in the direction of the bedding planes.

4.2. Inorganic element mobility

Conclusions from earlier investigations suggest the establishment of an overall geochemical equilibrium in BC (Wang et al., 2023; Honty et al., 2022; De Craen et al., 2004). This is supported by relatively similar geochemical parameters for BCPWs collected from different levels (Wang et al., 2023; Honty et al., 2022), with regard to e.g. pH, Na^+ and CO_3^{2-} concentrations. As mentioned above, the increasing trend of $NaHCO_3$, I^- and Cl^- with depth is explained by diffusion. Locally variable pore water compositions related to DOC, SO_4^{2-}, Fe and trace elements could be potentially correlated with biotic processes and DOM formation notably in BC regions of higher porosity. The potential role of microbial activity in this system is still under discussion (see e.g. (Wouters et al., 2013)). As already reported before, Morpheus-F8 pore waters contain beside elevated DOC levels as well significantly higher Fe-concentrations (~1 mg/L vs. ≤ 0.4 mg/L in other BCPWs, see Table 1). The observation of elevated concentrations of DOM and Fe in samples from the DB structure as compared to the other porewater samples can be taken as a further indication for the limited transfer/migration of DOM and inorganic ions from one layer to the other.

Lanthanides, U and Th abundant in natural samples have frequently been taken as analogues to radionuclide constituents of radioactive waste (Landström et al., 1995; Curtis et al., 2004; Montavon et al., 2022). Investigating their distribution in porewater/sediment systems can provide some insight into their mobility in a given system and might to some extent provide hints to the long-term behavior of waste derived radionuclides. Within the present study we try to interpret our data in this direction.

Fig. 3(a–c) shows lanthanide pattern where the concentrations in the samples are normalized to the content in the North American shale (North American Shale Composite; NASC; (DeVore)). Respective analyses of BCPWs and BC leachates have been performed within the present work (see Table 3). Lanthanide contents of the BC solid phases are taken from (De Craen, 2006; Clauer et al., 2022). It is noticeable that the normalized REE pattern differ from each other. For the BC solid phases (Fig. 3 a) we find a rather flat profile quite in agreement with a global average lanthanide abundance represented by NASC. Lanthanide pattern for the BC leachates and BCPWs (Fig. 3b and c) reveal conversely a relative depletion and enrichment of notably the heavy lanthanides, respectively. The shape of the profiles in BCPW samples could be the result of a preferential complexation of heavier lanthanides by humic/fulvic acids. Due to their smaller ionic radii concomitant with a higher charge density, complexation constants are higher (see e.g. (Sonke et al., 2006)). Enhanced complexation may be explained with the in general higher content of functional groups (carboxylic, phenolic groups) of BCPW humic/fulvic acids (~5-6 eq/kg) as compared to those of extracted OM (1.8 – 2.3 eq/kg) (Bruggeman et al., 2012). It is tempting to assume that the reverse slope of the lanthanide pattern in the extracts is the result of preferential leaching of heavy lanthanides from the REE bearing phases in the extracted BC colloidal matter and,

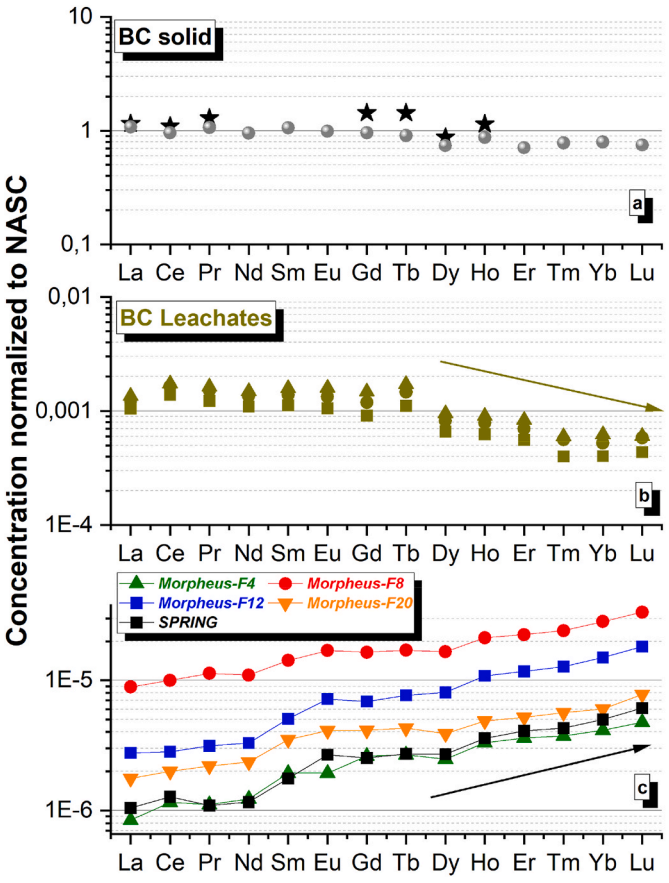

Fig. 3. Lanthanide pattern for a) BC solid phases (star symbol: data taken from Fig. 2 in (De Craen, 2006), sphere symbol: data taken from (Clauer et al., 2022)); b) for BC leachates and c) BCPW collected from different levels of the MORPHEUS piezometer; Lanthanide content in the solid phase in µg/g were normalized to the averaged Lanthanide content of the North American Shale Composite (NASC in µg/g); NASC values from (DeVore)).

thus, of chemical interactions between BCPW and BC bound OM. The previously discussed LC-OCD-UV-ICP-MS analyses evidence that significant fractions of yttrium and lanthanides (represented by La and Ce) as well as Th (and partly U) in BCPW and BC leachates are associated with colloidal matter, although with variable colloid size fractions.

In the following section we used our data in order to examine whether we can provide some information on the solid-liquid distribution of naturally abundant lanthanides, U and Th, and to compare those data with respective K_d-values derived from laboratory experiments with added lanthanides and actinides (Bruggeman et al., 2017). In a first instance we assume that the OM in the BC extracts corresponds predominantly to sorbed and immobile (i.e. captured in BC nanopores) OM (see as well Fig. 1 in (Durce et al., 2015)). DOM contained in BCPW within pores of the BC disks is considered to play a minor role. A second assumption made is that naturally abundant lanthanides and actinides in BCPW and BC extract are to a significant part associated to OM. This assumption appears to be reasonable considering a study performed by Bruggeman et al. (2010). They applied a "bottom-up" approach to simulate Eu(III) sorption to illite, taken as a proxy for the clay fraction in BC, in contact with BCPW and BC leachates. From their data, they conclude, that more than 50% of the sorbed Eu(III) could be attributed to binding to the "immobile" DOM (defined as the clay sorbed DOM plus the fraction >30 kDa in BCPW, which is not able to pass nanoporous clay layers by diffusion). Less than 50% of the sorbed Eu(III) is found sorbed to the clay minerals represented by illite.

We estimated the content of the naturally abundant trace elements Ce, Th and U in the BC leachates, by analyzing their concentration in a single extraction step from the BC solid sample (Table 2), where only 2-4% of OC was desorbed. As discussed above, Durce et al. (2015) state that only a part of the extractable OC can be leached in one step and increases to ~ 12% within multiple extraction steps. The analyzed Ce, Th and U concentrations are thus normalized to the extractable TOC of 12% acc. to (Durce et al., 2015) (see eq. SIF-1 in the SIF). Relating the trace element content in the extractable OM (which is considered to be bound to clay rock and thus insoluble and immobile acc. to (Durce et al., 2015)) to the respective concentrations in BCPWs as analyzed in the present work, we obtain distribution ratios for the naturally abundant trace elements Ce, Th and U between OM bound to clay rock and OM dissolved in BCPW, which we name *in-situ* $K_{d(OM)}$. The comparison of those ratios with K_d values selected by Bruggeman and Maes (Tables 3–8 in (Bruggeman et al., 2017)) for Eu(III) and actinide sorption to BC (log K_d = 3.5 – 4.5) results in similar values (see Fig. 4). A respective value for log(K_d(Eu(III)) derived from the sorption isotherm provided in Fig. 4 in Bruggeman et al. (2010) is ~4.1 and thus lies in the same range. The resemblance of all those K_d-values suggests that the immobile OM fraction significantly contributes to lanthanide, tri- and tetravalent actinide retention in BC.

The variation of our *in-situ* $K_{d(OM)}$ values for different BCPW samples is mainly due to their variable DOC content. It is furthermore noticeable that especially the *in-situ* $K_{d(OM)}$ values for Th in the low DOC BCPWs are significantly higher than the laboratory K_d-value range.

While the extractable OM represents only a minor fraction of the total OM in the clay rock, the potential contribution of main OM components in the solid phase (such as kerogen) to metal ion sorption can be estimated to be of low relevance. Kerogen of different types is characterized by low O/C ratios (~0.03 to 0.15 acc. to (Bruggeman et al., 2012)), corresponding to a low abundance of complexing functional groups. Respective O/C ratios for the BC humic acid fraction is at 0.32-0.46 and the easily extractable OM from BC is reported to consist essentially of humic acid (Bruggeman et al., 2012).

The assumption that trace elements only distribute between dissolved and extractable BC bound OM is certainly a simplification. As mentioned before, about 50% of Eu(III) can be expected to exist clay mineral surface bound in the Boom Clay system acc. to Bruggeman et al. (2010). If we multiply the value for the amount of adsorbed Ce in our study by a factor of 2, the resulting *in-situ log* $K_{d(OM)}$ values increase by only ~0.3. Still, *in-situ* $K_{d(OM)}$-values lie close to and within the range of recommended lab-K_d-values and may thus be taken as an independent confirmation.

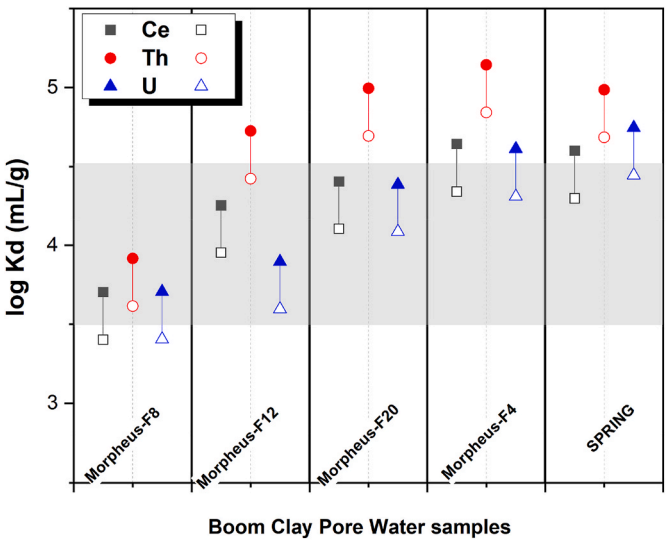

Fig. 4. In-situ log $K_{d(OM)}$ values for Ce, Th, U for various BCPW samples compared to log K_d values for Am(III), Eu(III), U(IV), Th(IV) determined in laboratory experiments (marked by the grey area) taken from the literature (Maes et al., 2011; Bruggeman et al., 2017); The variation of in-situ $K_{d(OM)}$-values (upper bound as filled symbol and lower bound as open symbol) for a given trace element and a specific BCPW are due to the bandwidth of TOC in the BC leachates after one leaching step and the total extractable TOC in the BC (see equation SIF-1 in the SIF, and the respective note there).

The association of uranium to OM – either clay mineral bound or dissolved OM – depends on redox state. As discussed before, in our solutions having had contact to air, U(VI) exists predominantly as carbonate complexes in solution. The similarity of *in-situ log* $K_{d(OM)}$ values for uranium, lanthanides and thorium suggests the presence of at least a part of uranium originally in the tetravalent state, when the BCPW and BC disks had been sampled from the BC formation. It is, however, also known from the literature that a $NaHCO_3$ solution is able to desorb U(VI) from mineral surfaces, while leaching of Ln(III) and notably Th(IV) by a $NaHCO_3$ solution will certainly be less efficient. Curtis et al. (2004) applied an extraction step with $NaHCO_3$ solution for their determination of *in-situ* K_d*-values* in an alluvial aquifer at a former U mill tailings site. The original chemical state of uranium under undisturbed BC conditions, thus, still needs to be clarified.

The role of colloidal FeOOH humic aggregates in BCPW and BC extracts observed in size-based LC-OCD and AsFlFFF analyses needs to be discussed in a similar way. Apparently, significant fractions of trace elements appear to be associated to such species, so that not only complexation with OM might be relevant. Currently, we assume that FeOOH humic aggregates form at least partly via Fe(II) oxidation due to the fact that size-based analyses are performed under aerobic conditions.

It is interesting to note, that previous investigations performed for sediment/groundwater system containing as well dissolved and sediment associated humic matter came to quite similar conclusions as made here (Geckeis et al., 2003; Bouby et al., 2012).

5. Conclusions

The present work deals with the characterization of natural Boom Clay pore waters (BCPW) originating from the HADES URL (MOL, Belgium) and Boom Clay solid leachates obtained in 15 mM $NaHCO_3$. The aim was to complement and/or to confirm some of the results obtained so far (Durce et al., 2015, 2018; Bruggeman et al., 2012) by using

complementary analytical techniques and to discuss possible inter-layer migration of OM nano entities in BCPW. Furthermore, the distribution of naturally abundant trace elements between BCPW and BC leachates is analyzed. Results are discussed in terms of providing insight into the role of OM for the geochemical behavior of such metal ions which are taken as chemical analogues to radioactive waste derived radionuclides.

Size characterization data for OM from different sampling sites as achieved within the present study is found in good agreement with earlier investigations performed with other analytical methods such as ultrafiltration and SEC at SCK CEN. AsFlFFF-UV and LC-OCD-UV-ICP-MS, however, provide size distributions with higher resolution and more details with regard to the distribution of naturally abundant trace metals within the clay sorbed and immobile OM (acc. to (Durce et al., 2015)) and dissolved DOM established over long time periods.

The small sized OM fraction with a size distribution centered at ~1.8 nm is considered mobile across sediment layers (horizontal direction and perpendicular to the bedding) in agreement with conclusions drawn by Durce et al. (2015). Variable tailings in the DOM size distributions found for different BC layers indicating the presence of larger sized DOM fractions are most pronounced for samples originating from or influenced by the DB structure (siltier zones). As those larger sized entities seem to be typical for the individual layers where the pore water came from, they can be considered as mobile in a horizontal direction within the respective layer. The significantly larger sized (DOM) species found in the BC leachates with sizes ranging up to ~ 30 nm can be considered as immobile as they are clearly associated with the solid clay phase under undisturbed BC conditions.

The association of naturally abundant polyvalent metal ions to DOM is clearly visible from LC-OCD-UV-ICP-MS chromatograms and consistent with investigations on the complexation of polyvalent actinides and fission products (e.g. Tc(IV)) with BC DOM (Maes et al., 2003, 2011). The fact, however, that association of metal ions is not uniform over the DOM size distribution, points to either some kind of preferential binding to specific DOM entities or to metal ion induced conformational changes of organic matter as already discussed earlier. The role of Fe needs to be further investigated. While it is assumed that Fe exists under the genuine pore water conditions in its reduced Fe(II) form, we assume, that during sampling, transport, handling and/or analysis in the lab oxidation occurs. Under such conditions solubility limits will be exceeded and FeOOH nanoparticles associated to DOM may form and contribute to the BC colloidal ensemble as well as to the distribution of trace elements within different colloidal size fractions. Experiments are currently underway to examine the possible impact of Fe-redox reactions in BCPW.

By analyzing the distribution of naturally abundant lanthanides and actinides in BC leachates and BCDOM, we derived *in-situ* $K_{d(OM)}$-values which lie close to or in the range of sorption coefficients obtained earlier for Eu(III), U(IV), Pu(IV) and Th(IV) in laboratory sorption studies with BC samples. Even though *in-situ* $K_{d(OM)}$-values are derived under certain simplified assumptions, their similarity to laboratory K_d-value ranges suggest that the OM leachable from BC (i.e. adsorbed and immobile OM acc. to (Durce et al., 2015)) has a significant impact on lanthanide and actinide retention in BC.

CRediT authorship contribution statement

Muriel Bouby: Conceptualization, Investigation, Methodology, Supervision, Validation, Visualization, Writing – original draft, Writing – review & editing. **Ugras Kaplan:** Investigation. **Frank W. Geyer:** Investigation. **Alexander Lunz:** Investigation. **Horst Geckeis:** Conceptualization, Supervision, Validation, Visualization, Writing – review & editing. **Stéphane Brassinnes:** Funding acquisition, Project administration, Resources, Validation, Writing – review & editing.

Declaration of competing interest

The authors declare that they have no known competing financial interests or personal relationships that could have appeared to influence the work reported in this paper.

Acknowledgments

This work was entirely funded by ONDRAF/NIRAS under contract CCHO2012-0422/00/00. We are grateful to two anonymous reviewers, who helped with their critical comments to improve the manuscript.

Appendix A. Supplementary data

Supplementary data to this article can be found online at https://doi.org/10.1016/j.apgeochem.2026.106807.

Data availability

Data will be made available on request.

References

Aiken, G.R., et al., 1985. Humic substances in soil, sediment, and water. Geochemistry, isolation and characterization. In: New-York, Chichester, Brisbane, Toronto, Singapore. A Wiley-InterscicencePublication John Wiley&sons, p. 692.
Aiken, G.R., 1985. Isolation and concentration techniques for aquatic humic substances. In: Aiken, G.R., et al. (Eds.), Humic Substances in Soil, Sediment and Water: Geochemistry, Isolation and Characterization. Wiley-Interscience, New York, pp. 363–385.
Avena, M.J., Vermeer, A.W.P., Koopal, L.K., 1999. Volume and structure of humic acids studied by viscometrypH and electrolyte concentration effects. Colloids Surf. A Physicochem. Eng. Asp. 151, 213–224.
Beckett, R., Jue, Z., Giddings, J.C., 1987. Determination of molecular weight distributions of fulvic and humic acids using flow field-flow fractionation. Environ. Sci. Technol. 21 (3), 289–295.
Benedetti, M.F., et al., 2003. The iron status in colloidal matter from the Rio Negro, Brasil. Colloids Surf. A Physicochem. Eng. Asp. 217 (1-3), 1–9.
Berden, M., Berggren, D., 1990. Gel filtration chromatography of humic substances in soil solutions using HPLC-determination of the molecular weight distribution. J. Soil Sci. 41 (1), 61–72.
Blanchart, P., et al., 2012. In situ and laboratory investigation of the alteration of Boom Clay (Oligocene) at the air-geological barrier interface within the mol underground facility (Belgium): consequences on kerogen and bitumen compositions. Appl. Geochem. 27 (12), 2476–2485.
Bouby, M., et al., 2011. Interaction of bentonite colloids with Cs, Eu, Th and U in presence of humic acid: a flow field-flow fractionation study. Geochem. Cosmochim. Acta 75 (13), 3866–3880.
Bouby, M., Finck, N., Geckeis, H., 2012. Flow field-flow fractionation (FlFFF) coupled to sensitive detection techniques: a way to examine radionuclide interactions with nanoparticles. Mineral. Mag. 76 (7), 2709–2721.
Bouby, M., Geckeis, H., Geyer, F.W., 2008. Application of asymmetric flow field-flow fractionation (AsFlFFF) coupled to inductively coupled plasma mass spectrometry (ICPMS) to the quantitative characterization of natural colloids and synthetic nanoparticles. Anal. Bioanal. Chem. 392 (7-8), 1447–1457.
Bruggeman, C., De Craen, M., 2012. Boom clay natural organic matter. Status Report 2011, SCK.CEN-ER206, External Report.
Bruggeman, C., Liu, D.J., Maes, N., 2010. Influence of boom clay organic matter on the adsorption of Eu3+ by illite-geochemical modelling using the component additivity approach. Radiochim. Acta 98 (9-11), 597–605.
Bruggeman, C., Maes, N., 2017. Radionuclide migration and retention in Boom Clay, SCK.CEN-ER0345, External report p. Tables 3-8.
Bruggeman, C., Maes, N., 2017. Radionuclide migration and retention in Boom Clay, SCK.CEN-ER0345, External report. Tables 3-8.
Chin, Y.P., Aiken, G., O'Loughlin, E., 1994. Molecular weight, polydispersity, and spectroscopic properties of aquatic humic substances. Environ. Sci. Technol. 28 (11), 1853–1858.
Chin, Y.P., Gschwend, P.M., 1991. The abundance, distribution, and configuration of porewater organic colloids in recent sediments. Geochem. Cosmochim. Acta 55 (5), 1309–1317.
Choppin, G.R., 1992. The role of natural organics in radionuclide migration in natural aquifer systems. Radiochim. Acta 58/59, 113–120.
Clapp, C.E., et al., 2001. Humic Substances and Chemical Contaminants. Soil Science Society of America, Inc.
Clauer, N., et al., 2022. Evaluation of a long-term thermal load on the sealing characteristics of potential sediments for a deep radioactive waste disposal. Sustainability 14 (21).
Curtis, G.P., et al., 2004. Comparison of in situ uranium KD values with a laboratory determined surface complexation model. Appl. Geochem. 19 (10), 1643–1653.
d'Orlyé, F., Varenne, A., Gareil, P., 2008. Determination of nanoparticle diffusion coefficients by Taylor dispersion analysis using a capillary electrophoresis instrument. J. Chromatogr. A 1204 (2), 226–232.

Davies, G., Ghabbour, E.A., Khairy, K.A., 1998. Humic Substances. Structures, Properties and Uses. Royal Society of Chemistry, UK.
De Craen, M., 2006. The Boom Clay geochemistry: natural evidence. In: Materials Research Society Symposium Proceedings.
De Craen, M., et al., 2004. Geochemistry of Boom Clay pore water at the Mol site. In: Scientific Report. SCK-CEN BLG-990.
De Craen, M., Moors, H., Verstricht, J., 2019. Description of the HADES piezometers used for the study of in situ Boom Clay pore water chemistry. Scientific Report. SCK•CEN ER-0329, SCK.CEN/12861301, 194 pages.
Deniau, I., et al., 2001. Morphological and chemical features of a kerogen from the underground Mol laboratory (Boom Clay formation, Oligocene, Belgium): structure, source organisms and formation pathways. Org. Geochem. 32 (11), 1343–1356.
DeVore, G.W., *Lanthanide Probes in Life, Chemical and Earth Sciences – Theory and Practice* 1989 Amsterdam: Elsevier.
Durce, D., et al., 2015. Partitioning of organic matter in Boom Clay: leachable vs mobile organic matter. Appl. Geochem. 63, 169–181.
Durce, D., et al., 2016. Alteration of the molecular-size-distribution of Boom Clay dissolved organic matter induced by Na+ and Ca2 +. J. Contam. Hydrol. 185-186, 14–27.
Durce, D., et al., 2018. Transport of dissolved organic matter in Boom Clay: size effects. J. Contam. Hydrol. 208, 27–34.
Gaffney, J.S., Marley, N.A., Clark, S.B., 1996. In: 651, A.S.S. (Ed.), Humic and Fulvic Acids. Isolation, Structure and Environmental Role. American Chemical Society, Washington, DC.
Geckeis, H., et al., 2002. Humic colloid-borne natural polyvalent metal ions: dissociation experiment. Environ. Sci. Technol. 36 (13), 2946–2952.
Geckeis, H., et al., 2003. Aquatic colloids relevant to radionuclide migration: characterization by size fractionation and ICP-mass spectrometric detection. Colloids Surf. A Physicochem. Eng. Asp. 217 (1-3), 101–108.
Ghabbour, E.A., Davies, G., 2000. Humic Substances. Versatile Components of Plants, Soil and Water. Royal Society of Chemistry, p. 341.
Ghosh, K., Schnitzer, M., 1980. Macromolecular structures of humic substances. Soil Sci. 129 (5), 266–276.
Giddings, J.C., Yang, F.J., Myers, M.N., 1976. Theoretical and experimental characterization of flow field-flow fractionation. Anal. Chem. 48 (8).
Gopalakrishnan, A., Bouby, M., Schäfer, A.I., 2023. Membrane-organic solute interactions in asymmetric flow field flow fractionation: interplay of hydrodynamic and electrostatic forces. Sci. Total Environ. 855.
Hasselöv, M., et al., 1999. Determination of continous size and trace element distribution of colloidal material natural water by on-line coupling of flow field-flow fractionation with ICP-MS. Anal. Chem. 71 (16), 3497–3502.
Hemes, S., et al., 2013. Variations in the morphology of porosity in the Boom Clay formation: insights from 2D high resolution BIB-SEM imaging and Mercury injection porosimetry. Geologie en Mijnbouw/Netherlands J. Geosci. 92 (4), 275–300.
Hemes, S., et al., 2015. Multi-scale characterization of porosity in Boom Clay (HADES-level, Mol, Belgium) using a combination of X-ray μ-CT, 2D BIB-SEM and FIB-SEM tomography. Microporous Mesoporous Mater. 208, 1–20.
Honty, M., et al., 2022. Boom Clay pore water geochemistry at the Mol site: experimental data as determined by in situ sampling of the piezometers. Appl. Geochem. 136.
Huber, S.A., et al., 2011. Characterisation of aquatic humic and non-humic matter with size-exclusion chromatography–organic carbon detection–organic nitrogen detection (LC-OCD-OND). Water Res. 45 (2), 879–885.
Huber, S.A., Frimmel, F.H., 1991. Flow injection analysis of organic and inorganic carbon in the low-ppb range. Anal. Chem. 63 (19), 2122–2130.
Ikeda, A., et al., 2009. Comparative Study of Uranyl(VI) and -(V) carbonato complexes in an aqueous solution. Inorg. Chem. 48 (13), 6321-6321.
Kawahigashi, M., Sumida, H., Yamamoto, K., 2005. Size and shape of soil humic acids estimated by viscosity and molecular weight. J. Colloid Interface Sci. 284 (2), 463–469.
Kim, J.I., Buckau, G., Zhuang, W., 1987. Humic colloid generation of transuranic elements in groundwater and their migration behaviour. In: Scientific Basis for Nuclear Waste Management X. Materials Research Soc, Pittsburgh, PA, USA; Boston, MA, USA.
Kirkland, J.J., Dilks, C.H., Rementer, S.W., 1992. Molecular-weight distributions of water-soluble polymers by flow field-flow fractionation. Anal. Chem. 64 (11), 1295–1303.
Laenen, B., 1997. The geochemical signature of relative sea-level cycles recognised in the Boom Clay. In: Aardkundige Mededelingen, pp. 61–82.
Landström, O., Tullborg, E.-L.E.-L., 1995. Interactions of trace elements with fracture filling minerals from the Äspö hard rock laboratory. In: *Technical Report*, S.-. Swedish Nuclear Fuel and Waste Management Co.
Lead, J.R., et al., 2000. Diffusion coefficients and polydispersities of the Suwannee river fulvic acid : comparison of fluorescence correlation spectroscopy, pulse-field gradient nuclear magnetic resonance, and flow field flow fractionation. Environ. Sci. Technol. 34 (16), 3508–3513.
Lou, T., Xie, H., 2006. Photochemical alteration of the molecular weight of dissolved organic matter. Chemosphere 65 (11), 2333–2342.
Maes, A., et al., 2003. Quantification of the interaction of Tc with dissolved Boom Clay humic substances. Environ. Sci. Technol. 37 (4), 747–753.
Maes, N., et al., 2011. A consistent phenomenological model for natural organic matter linked migration of Tc(IV), Cm(III), Np(IV), Pu(III/IV) and Pa(V) in the Boom Clay. Phys. Chem. Earth 36 (17-18), 1590–1599.
McCarthy, J.F., et al., 1998. Mobilization of transuranic radionuclides from disposal trenches by natural organic matter. J. Contam. Hydrol. 30 (1-2), 49–77.
Millipore, 2000. Millipore Data Sheet. Available from: www.millipore.com/techpublications/tech1/pf1172en00.
Müller, R.H., Schuhmann, R., 1996. Teilchengrössenmessung in Der Laborpraxis. Wissenschaftl. Verlagsgesellschaft mbH, Stuttgart, p. 38.
Montavon, G., et al., 2022. Uranium retention in a Callovo-Oxfordian clay rock formation: from laboratory-based models to in natura conditions. Chemosphere 299.
Moon, M.H., 1995. Effect of carrier solutions on particle retention in flow field-flow fractionation. Bull. Kor. Chem. Soc. 16 (7), 613–619.
Moon, J., Kim, S.H., Cho, J., 2006. Characterizations of natural organic matter as nano particle using flow field-flow fractionation. Colloids Surf. A Physicochem. Eng. Asp. 287 (1-3), 232–236.
Moulin, V., Ouzounian, G., 1992. Role of colloids and humic substances in the transport of radio-elements through the geosphere. Appl. Geochem. 179–186.
Ngo Manh, T., et al., 2001. Application of the flow-field flow fractionation (FFFF) to the characterisation of aquatic humic colloids . Evaluation and optimization of the method. Colloids Surf. A Physicochem. Eng. Asp. 181 (1-3), 289–301.
Pelekani, C., et al., 1999. Characterization of natural organic matter using high performance size exclusion chromatography. Environ. Sci. Technol. 33 (16), 2807–2813.
Perminova, I.V., et al., 2003. Molecular weight characteristics of humic substances from different environments as determined by size exclusion chromatography and their statistical evaluation. Environ. Sci. Technol. 37 (11), 2477–2485.
Piccolo, A., 2001. The supramolecular structure of humic substances. Soil Sci. 166 (11), 810–832.
Reiller, P.E., Buckau, G., 2012. Impacts of humic substances on the geochemical behaviour of radionuclides. In: Radionuclide Behaviour in the Natural Environment: Science, Implications and Lessons for the Nuclear Industry. Elsevier Ltd., pp. 103–160
Reszat, T., Hendry, M.J., 2009. Migration of colloids through nonfractured clay-rich aquitards. Environ. Sci. Technol. 43 (15), 5640–5646.
Roger, G.M., et al., 2010. Characterization of humic substances and polyacrylic acid: a high precision conductometry study. Colloids Surf. A Physicochem. Eng. Asp. 356 (1-3), 51–57.
Salah, S., Bruggeman, C., Maes, N., 2015. Uranium retention and migration behaviour in Boom Clay. In: Topical Report – Status 2014. SCK-CEN.
Schimpf, M.C.K., Gidding, J.C., 2000. In: Schimpf, M., Caldwell, K., Gidding, J.C. (Eds.), Field-Flow Fractionation Handbook. Wiley-Interscience, John Wiley & Sons Inc. New York, New York.
Schimpf, M.E., Wahlund, K.G., 1997. Asymmetrical flow field-flow fractionation as a method to study the behavior of humic acids in solution. J. Microcolumn Sep. 9 (7), 535–543.
Schimpf, M.E., Petteys, M.P., 1997. Characterization of humic material by flow field-flow fractionation. Colloids Surf., A : Physicochem. Eng. Aspects 120, 87–100.
Simpson, A.J., et al., 2002. Molecular structures and associations of humic substances in the terrestrial environment. Naturwissenschaften 89 (2), 84–88.
Siripinyanond, A., Barnes, R.M., Amarasiriwardena, D., 2002. Flow field-flow fractionation-inductively coupled plasma mass spectrometry for sediment bound trace metal characterization. J. Anal. At. Spectrom. 17 (9), 1055–1064.
Sonke, J.E., Salters, V.J.M., 2006. Lanthanide-humic substances complexation. I. Experimental evidence for a lanthanide contraction effect. Geochem. Cosmochim. Acta 70 (6), 1495–1506.
Striegel, A.M.K.J.J., Yau, W.W., Bly, D.D., 2009. Modern Size-Exclusion Liquid Chromatography. John Wiley & sons, Inc., Publication, p. 494.
Suffet, I.H., MacCarthy, P., 1989. Aquatic Humic Substances. Influent on Fate and Treatment of Pollutants. DC American Chemical Society, Washington.
Suteerapataranon, S., et al., 2006. Interaction of trace elements in acid mine drainage solution with humic acid. Water Res. 40 (10), 2044–2054.
Sutton, R., Sposito, G., 2005. Molecular structure in soil humic substances: the new view. Environ. Sci. Technol. 39 (23), 9009–9015.
Swift, R.S., 1999. Macromolecular properties of soil humic substances: fact, fiction, and opinion. Soil Sci. 164 (11), 790–802.
Tasi, A., et al., 2024. Degradation of the polyacrylonitrile-based UP2W material under cementitious conditions. Appl. Geochem. 169.
Taylor, H.E., et al., 1992. Inductively coupled plasma-mass spectrometry as an element-specific detector for field-flow fractionation particles separation. Anal. Chem. 64, 2036–2041.
Thurman, E.M., et al., 1982. Molecular size of aquatic humic substances. Org. Geochem. 4 (1), 27–35.
Van Geet, M., Bruggeman, C., De Craen, M., 2023. In: Li, X.L., et al. (Eds.), *Geological Disposal of Radioactive Waste in Deep Clay Formations: Celebrating 40 Years of RD& D in the Belgian URL HADES*, in *Geological Disposal of Radioactive Waste in Deep Clay Formations: 40 Years of RD& D in the Belgian URL HADES*. Geological Society of London. p. 0.
Van Geet, M., Maes, N., Dierckx, A., 2003. Characteristics of the Boom Clay Organic Matter, a Review. Geological Survey of Belgium, p. 298 (Professional paper 2003/1): pp. 1–23.
Vandenberghe, N., 1978. *Sedimentology of the Boom Clay (Rupelian) in Belgium.* . Verhandeling Koninklijke Academie Voor Wetenschappen, Letteren En Schone Kunsten Van België, XL147. Klasse Wetenschappen, pp. 1–137.
Wang, L., et al., 2023. Boom Clay pore-water geochemistry at the Mol site: chemical equilibrium constraints on the concentrations of major elements. Appl. Geochem. 148.
Wang, M., et al., 2020. Enhanced role of humic acid on the transport of iron oxide colloids in saturated porous media under various solution chemistry conditions. Colloids Surf. A Physicochem. Eng. Asp. 607, 125486.

Wijnhoven, J., et al., 1995. Hollow-fiber flow field-flow fractionation of polystyrene sulfonates. J. Chromatogr. A 699 (1-2), 119–129.
Wouters, K., et al., 2013. Evidence and characteristics of a diverse and metabolically active microbial community in deep subsurface clay borehole water. FEMS (Fed. Eur. Microbiol. Soc.) Microbiol. Ecol. 86 (3), 458–473.
Yu, L., et al., 2013. A critical review of laboratory and in-situ hydraulic conductivity measurements for the Boom Clay in Belgium. Appl. Clay Sci. 75-76, 1–12.